Periodic BEM and FEM-BEM coupling

Didier Clouteau, Marie Louise Elhabre, Denis Aubry

Periodic BEM and FEM-BEM coupling

Application to seismic behaviour of very long structures

D. Clouteau, M. L. Elhabre & D. Aubry

Abstract The main motivation of this work is the dynamic behavior of very long structures such as diaphragm and quay walls. Indeed despite a seemingly bi-dimensional or periodic geometry, a true three dimensional analysis has to be carried out since the seismic loading is fully three-dimensional. Unfortunately usual 3D models are not able to account for such large structures either from the theoretical or the numerical point of view. The development of a periodic approach accounting for general 3D loadings and using a Boundary Element Method is addressed in this paper. After introducing geometrical and functional frameworks, a generalised theory for periodicity fields and operators is given. It accounts for periodic domains and fields decompositions in view of a subdomain approach. Periodic boundary elements and special Green functions are then worked out. The third part points out some numerical validations and results issued from this theory applied to a real quay wall.

1 Introduction

The seismic behaviour of very long structures partially embedded in soil such as tunnels, diaphragm and quay walls is a major issue in earthquake engineering. The catastrophic failures of such structures that have occured in 1995 in Kobe [8] has pointed out the need of advanced modelling in this field to assert or modify usual designs based on simplified methods [11]. Beside the non-linear phenomena that often take place in the soil around these structures and which will not be accounted for in this paper, the effects of the dynamic interaction between the soil, the structure and the fluid together with the spatial variation of the incident fields have to be carefully addressed. Indeed, it has been shown that these interactions play a major role in the seismic behaviour of large buildings [16] or dams [14] modifying their dynamic response. It has also been shown that travelling incident waves can generate dangerous torsional motions in these structures.

For tunnels, diaphragm or quay walls, this last point may play a significant role for two reasons:

- these structures are very long compared to either the wave length or the correlation length of the seismic waves and in phase motion of such structures is very unlikely to occur during an earthquake,
- these structures are usually made of periodic cells connected with joints. The resistance of these joints is of critical importance for these structures especially when water is present. The maximum differential displacements or the coupling forces and moments inside these joints that are induced by spatially varying incidents fields have to be precisely known in order to design them properly.

At last for these structures the effect on the dynamic behaviour of the anchors usually added in the soil to ensure the static stability has to be investigated.

Accounting for all these aspects requires tri-dimensional models of these structures and the surrounding soil. Unfortunately mainly because of their very long size, such analyses can hardly be performed even using advanced numerical methods coupling FEM for the structure and BEM for the soil and the fluid together with powerful computers (see comparison results in Sect. 4.3). Moreover, in the limit case where these structures are supposed to be infinite, these methods lack for mathematical backgrounds to ensure their correctness.

To overcome these difficulties we propose to take advantage of the periodicity of these structures, building a numerical model dealing with only one cell on which almost classical numerical methods will be used. This generic model represents the overall structure submitted to any three-dimensional incident field provided the following hypotheses are assured:

- The structure is supposed to be infinite and periodic along one given direction denoted **d**. This is in fact a better hypothesis than accounting for a very small portion of it. We will give in the conclusion some ideas to account for the two ends of the structure.
- The soil is supposed to be horizontally layered, with no lateral heterogeneities. This is often the most valuable hypothesis that can be done on the soil regarding the available data in practical application. Let us remark that periodic lateral heterogeneities localised around the structure can be easily incorporated in the structure itself (this will be done for example for the anchors). For non periodic heterogeneities being either known or undeterministic one will refer to [25].
- The soil, the structure and the joints are supposed to have a visco-elastic behaviour so that superposition

D. Clouteau (✉), M. L. Elhabre, D. Aubry
LMSSM, Ecole Centrale de Paris-CNRS/URA 850,
92295 Chatenay-Malabry, France
e-mail: clouteau@mss.ecp.fr

The authors gratefully acknowledge the financial support of the Soletanche-Bachy company.

theorem can be applied. For local non-linear phenomena such as pounding or sliding along the joints, one will refer to [16].

Moreover in this paper we will only consider the case of deterministic seismic loadings consisting of plane waves. The case of stochastic incident fields is dealt in detail in [15] following the same framework. In addition one will restrict the theoretical developments to soil-structure interaction.

After some useful definitions and notations Sect. 2 will recall some classical results on periodic fields and operators and the associated Floquet transform which plays the same role as the usual Fourier transform. It is mainly based on Floquet pioneering work [21] on differential equations with periodic coefficients (see also [9]). It is then shown that one can restrict the analysis to a set of independant problems posed on a reference cell. Some mathematical details on these aspects can be found in [5, 24, 12] and more specifically in [15]. One can also refer to [7] as the methodology is quite similar to the one used for symmetry conditions.

In Sect. 3 we will see how these generic problems can be effectively solved using the classical substructuring technique [2, 4, 13] coupling Finite and Boundary Elements. For each of these methods one will address in detail the modification induced by the periodic conditions and especially the construction of periodic Green functions for an homogeneous or a stratified visco-elastic half-space (see [1, 23] for similar developments in other fields).

Section 4 will focus on numerical aspects related to the proposed method, its validation and its efficiency.

Section 5 will show a practical application of the method to a quay wall. We will concentrate here on the differential displacements between two neighboring panels.

2 The Floquet decomposition

In this section we will first present the three-dimensional problem we intend to solve together with the periodic assumption on its geometry. Then we will recall classical results concerning periodic functions and operators in one-dimension. These results will be extended to the 3D case leading to a set of independent problems posed on a generic cell.

2.1 Problem layout

Let us consider a very long structure modeled as an unbounded open set Ω_l with given elastic properties and which is embedded in an elastic half-space $\Omega_s = D - (D \cap \Omega_l)$, D being the half-space. $\Omega = \Omega_s \cup \Omega_l$ will denote the global domain. Ω_l is supposed to be periodic which means that there exists an elementary bounded cell $\tilde{\Omega}_l$ such that:

$$\tilde{\Omega}_l = \Omega_l \cap S_o \quad S_o = \{\mathbf{x} \in D \text{ such that } 0 < \mathbf{x} \cdot \mathbf{d} < L\} \tag{1}$$

$$\Omega_l = \bigcup_{n=-\infty}^{+\infty} \tilde{\Omega}_{ln} \quad \tilde{\Omega}_{ln} = \{\mathbf{x} \in D \text{ such that } \mathbf{x} - nL\mathbf{d} \in \tilde{\Omega}_l\} \tag{2}$$

The interfaces between Ω_l and Ω_s will be denoted Σ. The part of the boundary of each domain Ω_β on which Neumann boundary conditions are applied will be denoted $\Gamma_{\sigma\beta}$ (see Fig. 1).

For any displacement field $\mathbf{u}$ defined on Ω, $\mathbf{u}_\beta$ will denote its restriction to domain Ω_β, $\boldsymbol{\epsilon}(\mathbf{u}_\beta)$ and $\boldsymbol{\sigma}_\beta(\mathbf{u}_\beta)$ will be the strain and elastic stress tensors associated to these fields and $\mathbf{t}_\beta(\mathbf{u}_\beta) = \boldsymbol{\sigma}_\beta(\mathbf{u}_\beta)\mathbf{n}$ the traction vector on the boundary using the outer normal convention for n. Moreover one will use the following notations, $\mathbf{a}$ and $\mathbf{b}$ being any two vectors of $\mathbb{R}^3$ and $\mathbf{A}$ and $\mathbf{B}$ being any two tensors of $\mathbb{R}^3 \times \mathbb{R}^3$, $(\mathbf{Div}\,\mathbf{A})_j = \sum_i \partial_i A_{ji}$ is the divergence of the tensor, $\mathbf{a} \cdot \mathbf{b} = \sum_i a_i b_i$ is the scalar product, $\mathbf{A} : \mathbf{B} = \sum_{ij} A_{ij} B_{ij}$ is the contraction of two tensors and $(\mathbf{a} \otimes \mathbf{b})_{ij} = a_i b_j$ is the tensorial product.

Thanks to the linear hypothesis one will restrict the analysis to the dynamic pertubation of the static field due to dynamic loadings. This pertubation denoted $\mathbf{u}(\mathbf{x}, \omega)$ has to satisfy the Navier equation in Ω and boundary conditions on Γ_σ both written in the frequency domain for any circular frequency ω:

Problem 1 Find $\mathbf{u}(\mathbf{x}, \omega)$ defined on Ω satisfying:

$$\mathbf{Div}\,\boldsymbol{\sigma}(\mathbf{u}(\mathbf{x}, \omega)) = -\rho\omega^2 \mathbf{u}(\mathbf{x}, \omega) \quad \text{in } \Omega \tag{3}$$

$$\mathbf{t}(\mathbf{u})(\mathbf{x}, \omega) = \mathbf{0} \quad \text{on } \Gamma_\sigma \tag{4}$$

The dynamic loads consist in an incident field $\mathbf{u}_{\text{inc}}$ satisfying the Navier equation in D and the free-surface boundary conditions on ∂D. To avoid the definition of proper radiation conditions either in the half-space or in the structure, one will assume that some damping occurs in the materials modeled as a small imaginary part added to the elastic constants being either constant for hysteretic damping or proportional to ω for a viscous one. Thanks to this hypothesis, one can restrict the analysis to fields $\mathbf{u}_d = \mathbf{u} - \mathbf{u}_{\text{inc}r}$ having a finite energy on Ω i.e.:

$$\int_\Omega \{\mathbf{u}_d \cdot \overline{\mathbf{u}_d} + \boldsymbol{\sigma}(\mathbf{u}_d) : \overline{\boldsymbol{\epsilon}(\mathbf{u}_d)}\} \mathrm{d}V < +\infty \tag{5}$$

where $\overline{v}$ denote the complex conjugate of v, and where $\mathbf{u}_{\text{inc}r}$ is any smooth field on Ω such that $\mathbf{u}_{\text{inc}} - \mathbf{u}_{\text{inc}r}$ has a finite energy on Ω_s. Provided with hypothesis (5) one knows that Eqs. (3) and (4) have an unique solution for any given $\mathbf{u}_{\text{inc}}$ even though Ω_l is unbounded and $\mathbf{u}_{\text{inc}}$ has not a finite energy on Ω_s. However as Ω is unbounded, one has to find

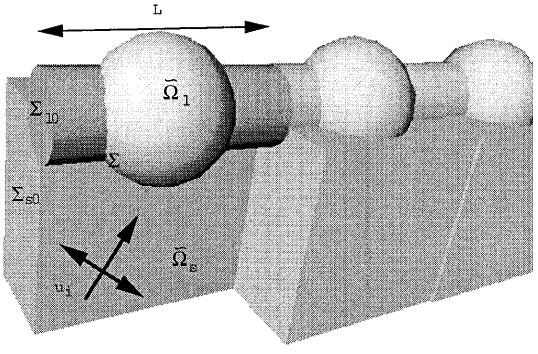

Fig. 1. Model layout

a way to build a numerical approximation of $\mathbf{u}$ on a functional space of finite dimension. In this section we will restrict the analysis to the reference cell $\tilde{\Omega} = \Omega \cup S_o$ using the Floquet transform.

2.2 1D Floquet periodicity

Before dealing with the 3D case, let us first recall some classical results due to Floquet [21]:

Definition 1 A complex valued function f defined on $\mathbb{R}$ is periodic of the second kind with period L and wavenumber κ if for any x in $\mathbb{R}$:

$$f(x+L) = \mathrm{e}^{-\mathrm{i}\kappa L} f(x) \tag{6}$$

This means that one can build this function for any x once it is known on $]0, L[$. This will be used to synthetize the solution on Ω once it will be known on $\tilde{\Omega}$, provided that this solution is periodic of the second kind. Unfortunately this is not true in general, but the following theorem will show that any function can be written as the superposition of a set of periodic functions of the second kind:

Theorem 1 Given a function f defined on $\mathbb{R}$ and a period L, its Floquet-transform $\tilde{f}$ defined on $]0, L[\times]-\pi/L, \pi/L[$ as follows:

$$\tilde{f}(\tilde{x}, \kappa) = \sum_{n=-\infty}^{+\infty} f(\tilde{x} + nL)\mathrm{e}^{\mathrm{i}n\kappa L} \tag{7}$$

is periodic of the second kind and for any $x = \tilde{x} + nL$, f may be recovered from its Floquet transform $\tilde{f}$ by:

$$f(x) = \frac{L}{2\pi} \int_{-\pi/L}^{\pi/L} \tilde{f}(\tilde{x}, \kappa)\mathrm{e}^{-\mathrm{i}n\kappa L}\, \mathrm{d}\kappa \tag{8}$$

Let us remark that $\tilde{f}$ may be build from $\hat{f}$ the Fourier Transform of f using the following formula:

$$\tilde{f}(\tilde{x}, \kappa) = \sum_{n=-\infty}^{+\infty} \hat{f}(\kappa + 2n\pi/L)\mathrm{e}^{-\mathrm{i}(\kappa+2n\pi/L)\tilde{x}} \tag{9}$$

$$\hat{f}(k) = \frac{1}{L}\int_0^L \tilde{f}(\tilde{x}, \kappa)\mathrm{e}^{\mathrm{i}k\tilde{x}}\, \mathrm{d}\tilde{x}, \quad k = \kappa + 2n\pi/L \tag{10}$$

These properties are of a great practical importance when dealing with differential operators with periodic coefficients. Indeed, let $\mathscr{A}$ be any differential operators with periodic coefficients i.e. satisfying for any u in $D(\mathscr{A})$ its domain of definition and for any $x \in \mathbb{R}$:

$$\mathscr{A}(x+L)u = \mathscr{A}(x)u \tag{11}$$

Then one can define the family of operators $\tilde{\mathscr{A}}_\kappa$ as the restriction of $\mathscr{A}$ on the reference cell $0 < x < L$ with additional periodic conditions of the second kind on the boundary of this cell, i.e. for any $0 < \tilde{x} < L$ and any functions $\tilde{u} \in D(\tilde{\mathscr{A}}_\kappa)$:

$$\tilde{\mathscr{A}}_\kappa(\tilde{x})\tilde{u} = \mathscr{A}(\tilde{x})u_r \text{ with } u_r(\tilde{x}) = \tilde{u}(\tilde{x}) \text{ and } u_r \in D(\mathscr{A}) \tag{12}$$

$$\tilde{u}(L) = \mathrm{e}^{-\mathrm{i}\kappa L}\tilde{u}(0) \tag{13}$$

Provided with this definition one can easily prove that:

$$(\tilde{\mathscr{A}}\tilde{u})(\tilde{x}, \kappa) = \tilde{\mathscr{A}}_\kappa(\tilde{x})\tilde{u}(\tilde{x}, \kappa) \tag{14}$$

for any $u \in D(\mathscr{A})$. As a consequence one can prove the following theorem:

Theorem 2 Let $\mathscr{A}$ be a periodic operator and f any function belonging to the image of $\mathscr{A}$. If Eq. (15) (resp. (16)) has an unique solution u in $D(\mathscr{A})$ (resp. $\check{u}$ in $D(\tilde{\mathscr{A}}_\kappa)$ for any $\kappa \in [-\pi/L, \pi/L[$):

$$\mathscr{A}u = f \tag{15}$$

$$\tilde{\mathscr{A}}_\kappa\check{u} = \tilde{f}, \check{u}(L) = \mathrm{e}^{-\mathrm{i}\kappa L}\check{u}(0) \tag{16}$$

then $\check{u} = \tilde{u}$, the Floquet transform of u.

This means that instead of solving Eq. (15) on $\mathbb{R}$ one can solve Eq. (15) on the generic cell for any κ such that $\tilde{f}$ does not vanish and then build solution u using the reconstruction formula (8).

The key point in using this theorem is that each equation must have a unique solution. In the following this will be achieved as long as damping is accounted for.

2.3 3D periodic domains

The aforementioned framework can be easily extended to our original three-dimensional problem having a periodicity L along one direction d ($\mathbf{x}$ is now a vector in $\mathbb{R}^3$). Using a simple separation of variables, it comes out that the analysis can be restricted to the generic domain $\tilde{\Omega}$. At this point, it is worth to notice that the boundary of $\tilde{\Omega}$ may be decomposed as follows:

$$\partial\tilde{\Omega} = \tilde{\Gamma}_\sigma \cup \Sigma_o \cup \Sigma_L \tag{17}$$

$$\Sigma_o = \{\mathbf{x} \in \Omega / \mathbf{x}\cdot\mathbf{d} = 0\}, \quad \Sigma_L = \{\mathbf{x} \in \Omega / \mathbf{x}\cdot\mathbf{d} = L\} \tag{18}$$

where $\tilde{\Gamma}_\sigma$ is the restriction of Γ_σ on the generic cell, and where Σ_o and Σ_L are additional boundaries on which periodic conditions are imposed. Provided with the Floquet transform of the incident field $\tilde{\mathbf{u}}_{\mathrm{inc}}(\tilde{\mathbf{x}}, \kappa)$ defined as follows:

$$\tilde{\mathbf{u}}_{\mathrm{inc}}(\tilde{\mathbf{x}}, \kappa) = \sum_{n=-\infty}^{+\infty} \mathbf{u}_i(\tilde{\mathbf{x}} + nL\mathbf{d})\mathrm{e}^{\mathrm{i}n\kappa L} \tag{19}$$

and separating Eqs. (3) and (4) into field equations in Ω_s and Ω_l, coupling equations on Σ and boundary conditions on $\Gamma_{\sigma s}$ and $\Gamma_{\sigma l}$, one has to solve the following generic problem for any $\kappa \in]-\pi/L, \pi/L[$:

Problem 2 Find $(\tilde{\mathbf{u}}_s(\tilde{\mathbf{x}}, \kappa), \tilde{\mathbf{u}}_l(\tilde{\mathbf{x}}, \kappa))$ defined on $\tilde{\Omega}_s \times \tilde{\Omega}_l$ satisfying:

$$\mathbf{Div}\,\sigma_s(\tilde{\mathbf{u}}_s - \tilde{\mathbf{u}}_{\mathrm{inc}}) = -\rho_s\omega^2(\tilde{\mathbf{u}}_s - \tilde{\mathbf{u}}_{\mathrm{inc}}) \quad \text{in} \quad \tilde{\Omega}_s \tag{20}$$

$$\mathbf{Div}\,\sigma_l(\tilde{\mathbf{u}}_l) = -\rho_l\omega^2\tilde{\mathbf{u}}_l \quad \text{in} \quad \tilde{\Omega}_l \tag{21}$$

$$\tilde{\mathbf{u}}_s = \tilde{\mathbf{u}}_l, \ \mathbf{t}_s(\tilde{\mathbf{u}}_s) + \mathbf{t}_l(\tilde{\mathbf{u}}_l) = \mathbf{0} \quad \text{on} \quad \tilde{\Sigma} \tag{22}$$

$$\mathbf{t}_\beta(\tilde{\mathbf{u}}_\beta) = \mathbf{0} \quad \text{on} \quad \tilde{\Gamma}_{\sigma\beta}, \beta \in \{s, l\} \tag{23}$$

$$\tilde{\mathbf{u}}_\beta(\mathbf{x}) = \mathrm{e}^{-\mathrm{i}\kappa L}\tilde{\mathbf{u}}_\beta(\mathbf{x} - Ld) \quad \text{for} \quad \mathbf{x} \in \Sigma_{\beta L}, \beta \in \{s, l\} \tag{24}$$

and the finite energy condition (5).

The global solution $\mathbf{u}(\mathbf{x})$, is recovered using formula (8) as follows:

$$\mathbf{u}_\beta(\mathbf{x} = \tilde{\mathbf{x}} + nL\mathbf{d}) = \frac{L}{2\pi}\int_{-\pi/L}^{\pi/L} \tilde{\mathbf{u}}_\beta(\tilde{\mathbf{x}}, \kappa)\mathrm{e}^{-\mathrm{i}n\kappa L}\,\mathrm{d}\kappa \tag{25}$$

Let us remark that when dealing with incident plane waves characterized by its horizontal wave number $\mathbf{k}_{\text{inc}}$ one has:

$$\hat{\mathbf{u}}_{\text{inc}}(k) \equiv \int_{-\infty}^{+\infty} \mathbf{u}_{\text{inc}}\mathrm{e}^{\mathrm{i}kx_d}\,\mathrm{d}x_d = \delta(k + \mathbf{k}_{\text{inc}} \cdot \mathbf{d})\hat{\mathbf{u}}_{\text{inc}}(-\mathbf{k}_{\text{inc}}) \tag{26}$$

with $x_d = \mathbf{x} \cdot \mathbf{d}$. This means that using Eq. (9) one gets:

$$\begin{aligned} &\tilde{\mathbf{u}}_{\text{inc}}(\tilde{\mathbf{x}}, \kappa) = \delta(\kappa - \kappa_i)\hat{\mathbf{u}}_i(\mathbf{k}_{\text{inc}})\mathrm{e}^{-\mathrm{i}\mathbf{k}_{\text{inc}}\cdot\tilde{\mathbf{x}}}, \\ &\qquad \kappa_i = -\mathbf{k}_{\text{inc}}.\mathbf{d} \bmod [2\pi/L] \end{aligned} \tag{27}$$

and as a consequence only one problem corresponding to $\kappa = \kappa_i$ has to be solved.

2.4
Remarks on the Floquet decomposition

Before trying to solve problem (2) on the generic cell using standard numerical techniques, let us draw some remarks:

- The only mathematical tool that is required to perform the Floquet decomposition is the theory of Fourier series. Indeed the decomposition formula (7) for a given $\tilde{\mathbf{x}}$ is nothing but the computation of the Fourier coefficient $f(\theta = \kappa L)$ of the series $\{f_n = f(\tilde{\mathbf{x}} + nL\mathbf{d})\}_{n\in\mathbf{Z}}$, reconstruction formula (8) being nothing but the general Fourier series decomposition.
- As a consequence of the previous remark, any numerical technique can be used together with the Floquet decomposition.
- The Floquet decomposition may be applied either in 1D, 2D or 3D.
- It may extended to 2D or 3D periodicity using a simple separation of variables.
- When the dimension of the periodicity is equal to the dimension of the space the reference cell is bounded otherwise it is not.
- The Floquet decomposition may be applied to 1D or 2D physical domains subjected to 3D loads. Indeed, 1D or 2D physical domains are periodic for any period L. Taking the limit when L tends to 0 gives the classical Fourier transform.
- The Floquet decomposition is a particular application of the group theory to physical problems governed by partial differential equations. For that reason it is very similar to the general framework proposed by Bossavit [7] for finite groups (plane symmetries, cyclic symmetries ...). As a consequence its implementation in numerical softwares that already account for these symmetries is very simple as we will see in the next section.

3
The numerical solution on the reference cell

As mentioned in Subsection 2.4, the Floquet decomposition applied to our original problem 1 is compatible with any numerical technique and it can take advantage of already existing methodologies developed to handle symmetries. For these reasons the numerical solution of problem 2 will be built using the classical domain decomposition approach [2] using FEM for the structure and BEM for the soil.

3.1
The subdomain approach

As $\tilde{\Omega}_l$ is bounded one can decompose the displacement field $\tilde{\mathbf{u}}_l$ on a given finite basis $\{\boldsymbol{\phi}_I(\kappa)\}_{I=1,N}$ that has to satisfy the periodicity conditions (24). Moreover let $\tilde{\mathbf{u}}_{do} + \tilde{\mathbf{u}}_{\text{inc}}$ and $\tilde{\mathbf{u}}_{dI}$ be fields defined in $\tilde{\Omega}_s$ satisfying the homogeneous Navier equation (20), the periodicity conditions (24), the homogeneous boundary conditions (23) and the following boundary conditions on $\tilde{\Sigma}$ the restriction of Σ on the reference cell:

$$\tilde{\mathbf{u}}_{dI} = \boldsymbol{\phi}_I \quad \text{on} \quad \tilde{\Sigma} \tag{28}$$

$$\tilde{\mathbf{u}}_{do} + \tilde{\mathbf{u}}_{\text{inc}} = \mathbf{0} \quad \text{on} \quad \tilde{\Sigma} \tag{29}$$

Then one has the following decomposition either in $\tilde{\Omega}_l$ or in $\tilde{\Omega}_s$:

$$\tilde{\mathbf{u}}_l(\tilde{\mathbf{x}}) = \sum_{I=1}^{N} c_I\boldsymbol{\phi}_I(\tilde{\mathbf{x}}) \tag{30}$$

$$\tilde{\mathbf{u}}_s(\tilde{\mathbf{x}}) = \tilde{\mathbf{u}}_{\text{inc}}(\tilde{\mathbf{x}}) + \tilde{\mathbf{u}}_{do}(\tilde{\mathbf{x}}) + \sum_{I=1}^{N} c_I\tilde{\mathbf{u}}_{dI}(\tilde{\mathbf{x}}) \tag{31}$$

At last, using a standard Galerkin approximation procedure in writing the equilibrium of $\tilde{\Omega}_l$ in a weak sense for any $\boldsymbol{\phi}_J$ in the basis, one comes up with the following linear system:

$$\left\{\mathbf{K}(\kappa) - \omega^2\mathbf{M}(\kappa) + \mathbf{K}_s(\omega, \kappa)\right\}\mathbf{c}(\omega, \kappa) = \mathbf{F}_s(\omega, \kappa) \tag{32}$$

where:

$$\begin{aligned} K_{IJ} &= \int_{\tilde{\Omega}_l} \boldsymbol{\sigma}_l(\boldsymbol{\phi}_I) : \boldsymbol{\epsilon}(\overline{\boldsymbol{\phi}_J})\mathrm{d}V, \quad M_{IJ} = \int_{\tilde{\Omega}_l} \rho_l\boldsymbol{\phi}_I \cdot \overline{\boldsymbol{\phi}_J}\,\mathrm{d}V \\ K_{sIJ} &= \int_{\tilde{\Sigma}} \mathbf{t}_s(\tilde{\mathbf{u}}_{dI}) \cdot \overline{\boldsymbol{\phi}_J}\,\mathrm{d}S, \\ F_{sJ} &= -\int_{\tilde{\Sigma}} (\mathbf{t}_s(\tilde{\mathbf{u}}_{\text{inc}}) + \mathbf{t}_s(\tilde{\mathbf{u}}_{do})) \cdot \overline{\boldsymbol{\phi}_J}\,\mathrm{d}S \end{aligned} \tag{33}$$

In order to solve this equation for any ω and κ one has first to compute the unknown traction fields $\mathbf{t}_s(\tilde{\mathbf{u}}_{dI})$ and $\mathbf{t}_s(\tilde{\mathbf{u}}_{do})$. The next subsection is devoted to this task using a boundary element technique. Another issue consists in building the basis $\boldsymbol{\phi}_I(\kappa)$ using a standard Finite Element technique and will be presented in 3.3. The main point is thus that the classical domain decomposition approach is then extended to the case of periodic domain very easily.

3.2
Periodic boundary elements

We propose here to compute the fields $\tilde{\mathbf{u}}_{dI}$ and $\tilde{\mathbf{u}}_{do}$, solutions of local boundary value problems of the following type:

Problem 3 Find $\mathbf{u}$ in $\tilde{\Omega}_s$ such that:

$$\mathbf{Div}\,\boldsymbol{\sigma}(\mathbf{u}) = -\rho\omega^2\mathbf{u} \quad \text{in} \quad \tilde{\Omega}_s \tag{34}$$

$$\mathbf{u} = \mathbf{u}_o \quad \text{on} \quad \tilde{\Sigma} \tag{35}$$

$$\mathbf{t}_s(\mathbf{u}) = \mathbf{0} \quad \text{on} \quad \tilde{\Gamma}_{\sigma s} \tag{36}$$

$$\mathbf{u}(\mathbf{x}) = \mathrm{e}^{-\mathrm{i}\kappa L}\mathbf{u}(\mathbf{x} - L\mathbf{d}) \quad \text{for} \quad \mathbf{x} \in \Sigma_{sL} \tag{37}$$

using a Boundary Element Method [6] based on classical integral equations [17]. However as neither the left periodic interface Σ_{so} nor the right one Σ_{sL} is bounded (see Fig. 1), a standard BEM cannot be directly used. Moreover, although it may be possible to account for periodic conditions in a BEM framework, this would still require heavy developments in existing computer codes. To avoid these drawbacks, let us use the following periodic fundamental solutions and integral operators [1, 23, 12]:

Definition 2 $\mathbf{U}_s^G$ being the Green tensor of the elastic half-space D, let $\tilde{\mathbf{U}}_s^G$ be the periodic Green Tensor and $\tilde{\mathscr{U}}_s^G$ the associated integral operator defined as follows:

$$\tilde{\mathbf{U}}_s^G(\tilde{\mathbf{x}}, \tilde{\mathbf{y}}; \kappa) = \sum_{-\infty}^{+\infty} \mathrm{e}^{\mathrm{i}n\kappa L}\mathbf{U}_s^G(\tilde{\mathbf{x}}, \tilde{\mathbf{y}} + nL\mathbf{d}) \tag{38}$$

$$\tilde{\mathscr{U}}_s^G(q)(\tilde{\mathbf{y}}) = \int_{\tilde{\Sigma}} \tilde{\mathbf{U}}_s^G(\tilde{\mathbf{x}}, \tilde{\mathbf{y}})\tilde{\mathbf{q}}(\tilde{\mathbf{x}})\mathrm{d}S(\tilde{\mathbf{x}}) \tag{39}$$

From these definitions one can easily remark that $\tilde{\mathbf{U}}_s^G(\tilde{\mathbf{x}}, \tilde{\mathbf{y}})$ and $\tilde{\mathscr{U}}_s^G(\tilde{\mathbf{q}})$ are periodic of the second kind with respect to $\tilde{\mathbf{y}}$ and with wavenumber equal to κ. Moreover one can remark that locally $\tilde{\mathbf{U}}_s^G$ has the same singularities as $\mathbf{U}_s^G$. As a consequence problem 3 is equivalent to the following Boundary integral equation where the integral is only on the bounded interface $\tilde{\Sigma}$ as periodic boundary conditions are automatically accounted for:

Problem 4 Find $\tilde{\mathbf{q}}$ on $\tilde{\Sigma}$ satisfying for any $\tilde{\mathbf{y}} \in \tilde{\Sigma}$:

$$\int_{\tilde{\Sigma}} \tilde{\mathbf{U}}_s^G(\tilde{\mathbf{x}}, \tilde{\mathbf{y}})\tilde{\mathbf{q}}(\tilde{\mathbf{x}})\mathrm{d}S(\tilde{\mathbf{x}}) = \mathbf{u}_o(\tilde{\mathbf{y}}) \tag{40}$$

The tractions $\mathbf{t}_s(u)$ needed in Eqs. (34) and (34) are then given for any $\tilde{\mathbf{y}} \in \tilde{\Sigma}$:

$$\mathbf{t}_s(u)(\tilde{\mathbf{y}}) = -1/2\tilde{\mathbf{q}}(\tilde{\mathbf{y}}) + \int_{\tilde{\Sigma}} \mathbf{t}_s(\tilde{\mathbf{U}}_s^G)(\tilde{\mathbf{x}}, \tilde{\mathbf{y}})\tilde{\mathbf{q}}(\tilde{\mathbf{x}})\mathrm{d}S(\tilde{\mathbf{x}}) \tag{41}$$

The numerical solution of this integral equation may be computed using either standard three-dimensional BEM using collocation procedure or Symmetric Galerkin Boundary Elements. In both cases, the only modification consists in computing the periodic Green tensors using formula (38) and integrate it on the boundary elements. Because of the singularity of the Green tensors around $x = y$ one will use the following procedure : let us consider first constant shape function for $\tilde{\mathbf{q}}$ and collocation point at the baricenter of each element. Then one has to compute the following 3×3 matrix:

$$\mathsf{U}_{EF} = \int_E \tilde{\mathbf{U}}_s^G(\tilde{\mathbf{x}}, \tilde{\mathbf{y}}_F)\mathrm{d}S \tag{42}$$

As long as removing the term $n = 0$, the series (38) converges uniformly for any $(\tilde{\mathbf{x}}, \tilde{\mathbf{y}})$, one can invert the summation in Eq. (38) and the integral in Eq. (42) to get the following expression of U_{EF}:

$$\mathsf{U}_{EF} = \sum_{-\infty}^{+\infty} \mathrm{e}^{\mathrm{i}n\kappa L}\mathsf{U}_{EF}^n, \;\; \mathsf{U}_{EF}^n = \int_E \tilde{\mathbf{U}}_s^G(\tilde{\mathbf{x}}, \tilde{\mathbf{y}}_F + nL\mathbf{d})\mathrm{d}S \tag{43}$$

In this sum the singular terms arising only for $n = 0$ are nothing but the usual 3D-BEM terms and are handled using classical techniques (either singular integral procedures or regularisation techniques for homogeneous [6] or stratified domains [3]). The other terms are regular and can be computed using standard gaussian formula. The infinite sum is truncated when convergence is reached [19, 20](see Sect. 4.1).

3.3
The periodic structure

When dealing with Finite Elements, the computation of the matrices K and M defined in Eq. (33) is not straightforward as $\boldsymbol{\phi}_I$ depends explicitly on κ (See [22] for periodic FEM). Using classical dynamic substructuring it is shown that K and M have an explicit dependence on κ by an extension of the Craig-Bampton [18] substructuring technique. It consists in the expansion of the displacement field of the structure $\tilde{\Omega}_l$ on dynamic eigenmodes $\boldsymbol{\phi}_\alpha$ with a fixed interfaces and on static modes ($\omega = 0$ in Eq. (21)) generated by given displacements of the interface (practically unitary displacements of the nodes belonging to the interface). In the present case the interface consists of three parts $\tilde{\Sigma}$, Σ_{lo} and Σ_{lL}. Let us first call $\boldsymbol{\psi}_\beta$ the static modes that vanish on Σ_{lo} and Σ_{lL}. As a consequence they satisfy the periodic condition (24). Then, as long as the structure is periodic, one can find couples of the remaining static modes $(\boldsymbol{\varphi}_{o\gamma}, \boldsymbol{\varphi}_{L\gamma})$ satisfying:

$$\boldsymbol{\varphi}_{o\gamma}(\tilde{\mathbf{x}}) = \boldsymbol{\varphi}_{L\gamma}(\tilde{\mathbf{x}} + L\mathbf{d})\boldsymbol{\varphi}_{o\gamma}(\tilde{\mathbf{x}} + L\mathbf{d}) = \boldsymbol{\varphi}_{L\gamma}(\tilde{\mathbf{x}}) = \mathbf{0} \quad \text{for } \tilde{\mathbf{x}} \in \Sigma_{lo} \tag{44}$$

One can then build new static modes $\tilde{\boldsymbol{\varphi}}_\gamma$ combining these ones such that they also satisfy the periodic condition (24):

$$\tilde{\boldsymbol{\varphi}}_\gamma(\tilde{\mathbf{x}}) = \mathrm{e}^{\mathrm{i}\kappa L/2}\boldsymbol{\varphi}_{o\gamma}(\tilde{\mathbf{x}}) + \mathrm{e}^{-\mathrm{i}\kappa L/2}\boldsymbol{\varphi}_{L\gamma}(\tilde{\mathbf{x}}) \tag{45}$$

As the stiffness and mass matrices K^o and M^o expressed on the static and dynamic mode basis satisfy:

$$\begin{aligned} &\boldsymbol{\phi}_{\alpha'}^{\mathrm{T}}\mathsf{K}^o\boldsymbol{\phi}_\alpha = \omega_\alpha^2\boldsymbol{\phi}_{\alpha'}^{\mathrm{T}}\mathsf{M}^o\boldsymbol{\phi}_\alpha = \omega_\alpha^2\delta_{\alpha\alpha'}, \\ &\boldsymbol{\phi}_\alpha^{\mathrm{T}}\mathsf{K}^o\boldsymbol{\psi}_\beta = \boldsymbol{\phi}_\alpha^{\mathrm{T}}\mathsf{K}^o\boldsymbol{\varphi}_\gamma = 0 \end{aligned} \tag{46}$$

one is then able to compute easily the stiffness and mass matrices arising in Eq. (32) as a function of the FEM stiffness and mass matrices K^o and M^o, using a simple projection technique on this new basis. For example,

denoting $\lambda = \mathrm{e}^{-\mathrm{i}\kappa L/2}$, the stiffness coefficient for two modes $\tilde{\boldsymbol{\varphi}}_\gamma(\tilde{\mathbf{x}})$ and $\tilde{\boldsymbol{\varphi}}_{\gamma'}(\tilde{\mathbf{x}})$ is then given by:

$$\mathsf{K}_{\alpha\alpha'} = \omega_\alpha^2 \mathsf{M}_{\alpha\alpha'} = \omega_\alpha^2 \delta_{\alpha\alpha'} \quad \mathsf{K}_{\alpha\beta} = \mathsf{K}_{\alpha\gamma} = 0$$
$$\mathsf{K}_{\beta\beta'} = \boldsymbol{\psi}_\beta^{\mathrm{T}} \mathsf{K}^o \boldsymbol{\psi}_{\beta'} \quad \mathsf{M}_{\beta\beta'} = \boldsymbol{\psi}_\beta^{\mathrm{T}} \mathsf{M}^o \boldsymbol{\psi}_{\beta'} \quad \mathsf{M}_{\alpha\beta} = \boldsymbol{\phi}_\alpha^{\mathrm{T}} \mathsf{M}^o \boldsymbol{\psi}_\beta \tag{47}$$

$$\mathsf{K}_{\gamma\beta} = \lambda^{-1} \boldsymbol{\varphi}_{o\gamma}^{\mathrm{T}} \mathsf{K}^o \boldsymbol{\psi}_\beta + \lambda \boldsymbol{\varphi}_{L\gamma}^{\mathrm{T}} \mathsf{K}^o \boldsymbol{\psi}_\beta$$
$$\mathsf{M}_{\gamma\beta} = \lambda^{-1} \boldsymbol{\varphi}_{o\gamma}^{\mathrm{T}} \mathsf{M}^o \boldsymbol{\psi}_\beta + \lambda \boldsymbol{\varphi}_{L\gamma}^{\mathrm{T}} \mathsf{M}^o \boldsymbol{\psi}_\beta \tag{48}$$
$$\mathsf{M}_{\gamma\alpha} = \lambda^{-1} \boldsymbol{\varphi}_{o\gamma}^{\mathrm{T}} \mathsf{M}^o \boldsymbol{\phi}_\alpha + \lambda \boldsymbol{\varphi}_{L\gamma}^{\mathrm{T}} \mathsf{M}^o \boldsymbol{\phi}_\alpha$$

$$\mathsf{K}_{\gamma\gamma'} = \lambda^{-2} \boldsymbol{\varphi}_{o\gamma}^{\mathrm{T}} \mathsf{K}^o \boldsymbol{\varphi}_{o\gamma'} + (\boldsymbol{\varphi}_{o\gamma}^{\mathrm{T}} \mathsf{K}^o \boldsymbol{\varphi}_{L\gamma'} + \boldsymbol{\varphi}_{L\gamma}^{\mathrm{T}} \mathsf{K}^o \boldsymbol{\varphi}_{o\gamma'}) + \lambda^2 \boldsymbol{\varphi}_{L\gamma}^{\mathrm{T}} \mathsf{K}^o \boldsymbol{\varphi}_{L\gamma'} \tag{49}$$
$$\mathsf{M}_{\gamma\gamma'} = \lambda^{-2} \boldsymbol{\varphi}_{o\gamma}^{\mathrm{T}} \mathsf{M}^o \boldsymbol{\varphi}_{o\gamma'} + (\boldsymbol{\varphi}_{o\gamma}^{\mathrm{T}} \mathsf{M}^o \boldsymbol{\varphi}_{L\gamma'} + \boldsymbol{\varphi}_{L\gamma}^{\mathrm{T}} \mathsf{M}^o \boldsymbol{\varphi}_{o\gamma'}) + \lambda^2 \boldsymbol{\varphi}_{L\gamma}^{\mathrm{T}} \mathsf{M}^o \boldsymbol{\varphi}_{L\gamma'}$$

In this manner it is clearly seen that the stiffness and the mass matrices have an explicit expression with respect to λ and thus need not be computed each time.

4 The numerical aspects

In Subsection 3.2 we saw that the numerical solution of the periodic integral equation which is the core of the method is handled using standard three-dimensional BEM but with an additional sum on the source terms as expressed in Eq. (43). Numerically this infinite sum is replaced by a finite one:

$$\mathsf{U}_{EF} = \sum_{-N_c}^{+N_c} \mathrm{e}^{\mathrm{i}n\kappa L} \mathsf{U}_{EF}^n \tag{50}$$

N_c being large enough to ensure the convergence. The aim of this section is on the first hand to examine this convergence and on the second one to validate the periodic formulation. In fact we will examine the convergence and the accuracy of the terms of the impedance matrix as given in formula (34).

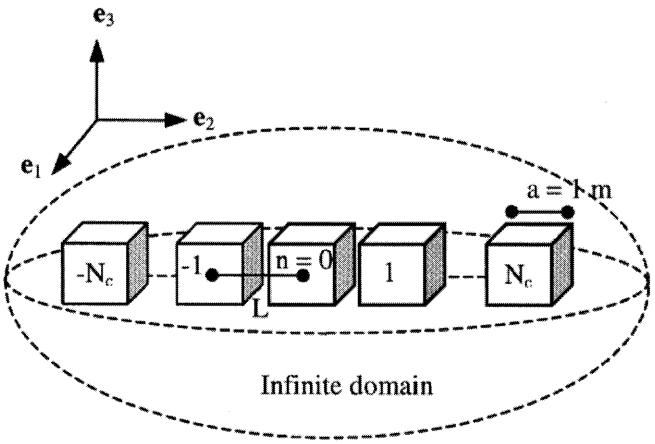

Fig. 2. Model layout for numerical validation

Let us consider a set of identical and regularly spaced rigid cubes lying in an infinite homogeneous space as shown in Fig. 2. As these cubes are rigid they have only six degrees of freedom, the impedance matrix being a 6×6 matrix. The cubes dimension denoted by a is set to one meter ($a = 1$ m) and the distance L between their gravity centres is the geometric periodicity length.

On Fig. 3 we have plotted the real and the imaginary parts of the impedance in the e_1e_1 direction. One can notice that convergence becomes slower when the cubes get closer. Two extreme cases are shown: one deals with very distant cubes ($a = 1$ m, $L = 50$ m) for which N_c can be set equal to five, the other one corresponds to side by side cubes ($a = L = 1$ m) where N_c has to be greater than 30.

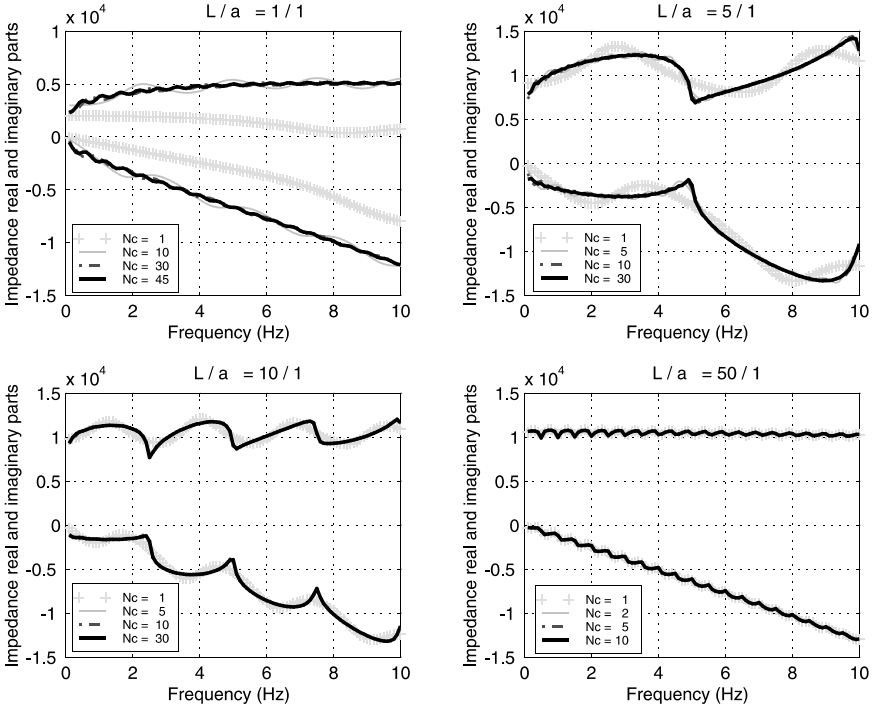

Fig. 3. Convergence thresholds for impedances

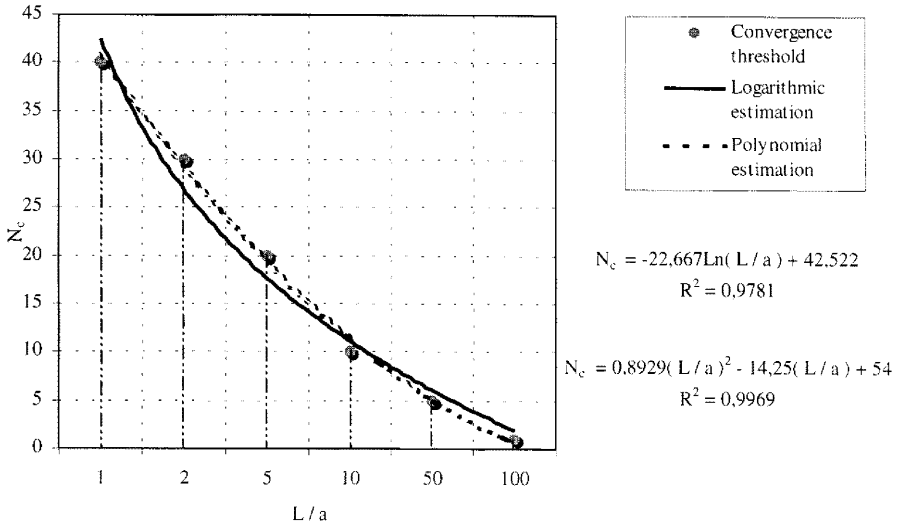

Fig. 4. Estimation of the convergence thresholds

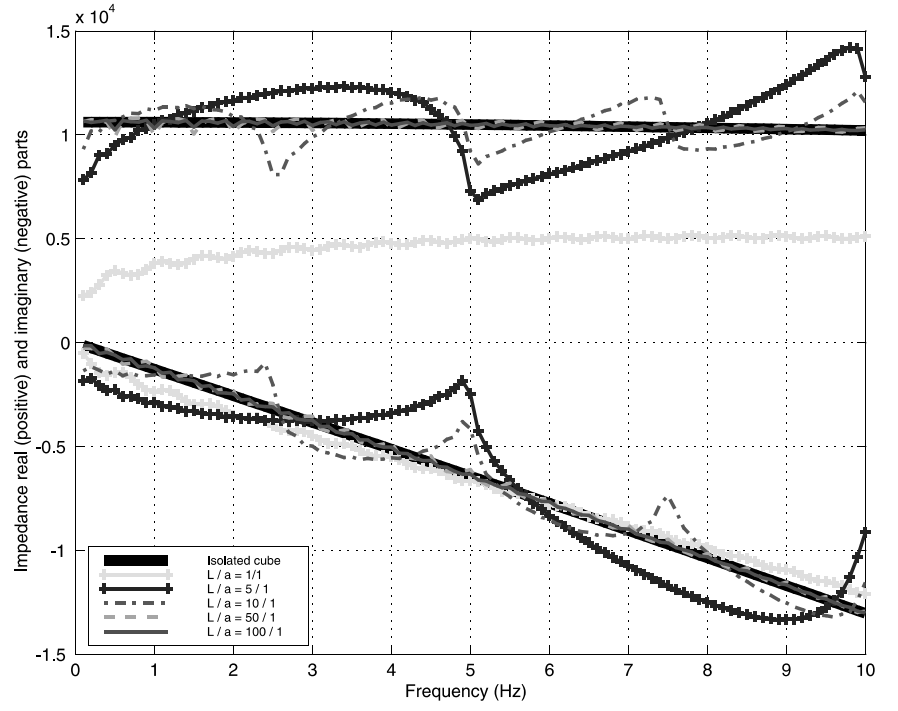

Fig. 5. Influence of the Periodicity length (L)

4.1 Convergence

The dots on Fig. 4 show the convergence thresholds, as computed above, plotted for several dimensionless ratios L/a. These thresholds seem to have a second order polynomial variation function of the ratio L/a more convincing than a logarithmic one according to the correlation factor R^2 shown on this graph.

4.2 Effect of the periodicity length

Once convergence being ensured, one can observe the influence of the periodicity length. Figure 5 gives the impedance in the e_1e_1 direction for several values of L. The impedance of an isolated cube lying in the same infinite space is also plotted (black thick line). As L grows, the curves of the periodic set get closer to the isolated one enhancing the fact that when the distance between cubes increases, their mutual influence varies in the opposite way and they behave as isolated cubes.

4.3 Validation and efficiency

Several validation have been performed comparing the periodic results with either 2D or 3D results. As an example we show on Fig. 6 the impedance of side by side case using two approaches: the classical BEM (dotted curves) and the periodic one (continuous curves). The correlation between the two approaches is quite convincing. Let us remark that in order to reach convergence for

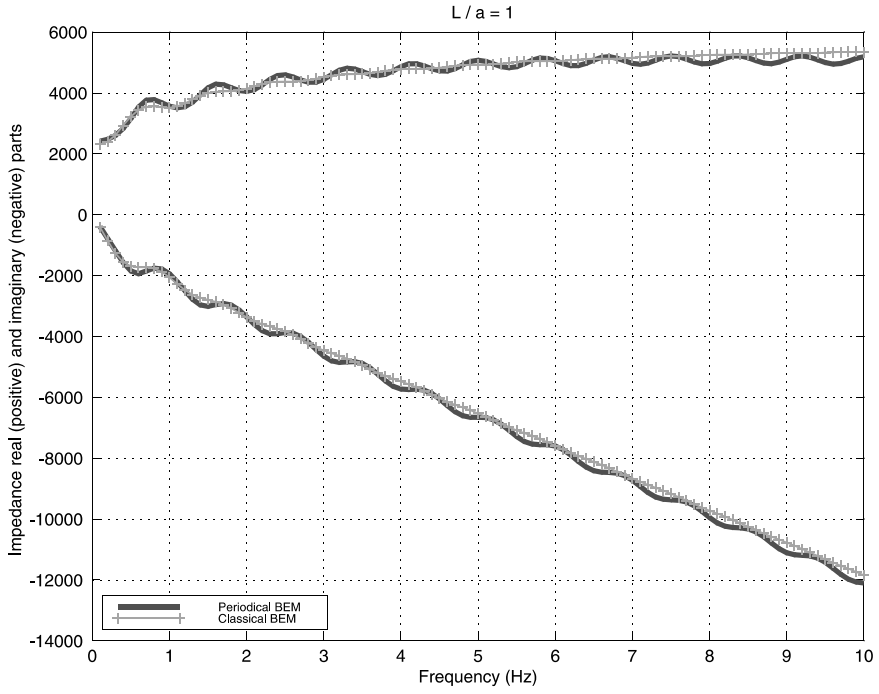

Fig. 6. Validation example in a quasi-2D case

3D model one has to use a very large mesh including about 100 cubes whereas in the periodic case only one cube has been meshed.

The gain in computational time between these two models is of about fifty and reaches several thousands for disk requirements. Indeed with the periodic approach the size of files needed is the one corresponding to one generic cell whatever N_c should be which is clearly not the case in the classical approach where the size is proportional to N_c^2.

As mentioned in Sect. 3.2 periodic BEM can be easily implemented in any existing BEM code. We have shown in this section some validations of this approach and its efficiency compared to a full 3D approach.

5 Application

We present here a study on the dynamic behaviour of diaphragm and quay walls. These retaining walls (see Fig. 7) which can reach 1 kilometer long, are made of identical panels of about six meters long connected with joints. The panels are anchored using tiebacks. Their static behavior is relatively well-known, which is not the case concerning their dynamic one. In fact when earthquake occurs, waves propagate in many directions. For inclined incident waves or surface incident waves, the panels will not vibrate in phase creating differential displacement between panels which may lead to water infiltration and other dangerous phenomena. The presence of joints and anchors as well as the 3D characteristics of the loadings require a full 3D analysis. Regarding to the dimensions of such structures a Finite Element model would lead to a huge number of degrees of freedom. A Boundary Element Method is more suitable since only the interfaces between domains need to be meshed. Let us remark that for an industrial case and even using BEM and a high performance supercomputer we were able to model only six panels using a full 3D approach; which is clearly not enough to account for interactions effects between panels.

The periodic approach proposed in this paper is particularly suited for these analyses as quay walls are periodic, the generic cell made of one panel with its anchors,

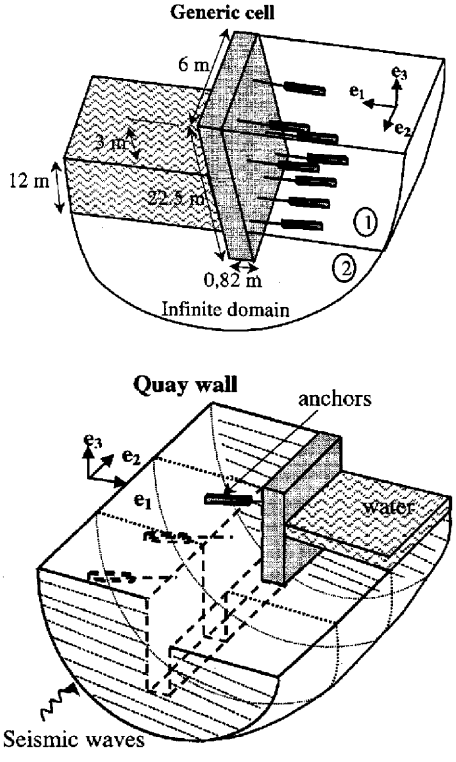

Fig. 7. An example of a quay wall and its generic cell

the corresponding slice of soil and eventually the fluid as shown on Fig. 5. The panel is a concrete thick plate. Three inclined anchoring beds reinforce its stability. The panel lies in a linear elastic stratified halfspace made of two layers referred to by numbers 1 and 2. The loading is a plane shear wave propagating vertically with a polarisation in the e_1 direction. In order to make a comparative study, we have computed several models including or not the anchors and the water (see Fig. 5).

- case AW (Anchors and Water) will denote the case with Anchors and Water,
- case AN the same case without water,
- case FW will stand for Free of Anchors with Water,
- case FN standing for Free of Anchors with No water.

As shown in Subsection 3.3 a Finite Element analysis is required for the structure (the free panel in cases FW and FN and with the anchors in cases AW and AN) in order to determine the displacement fields decomposition (see Eq. (31)). This leads to the eigenmodes $\{\boldsymbol{\phi}_I(\kappa)\}_{I=1,N}$ where N is set to 20. The choice of this basis dimension is made according either to an a posteri criterium: we verify that the participation of the last eigenmode taken into account (ϕ_{20}) is negligible, or an a priori criterium where the last eigenmode frequency must be at least 2.5 time the maximum of the frequency range ([0.1 Hz, 12.5 Hz] in our study). Our choice fulfills the two criteria.

Another preliminary verification was made concerning the number of cells (threshold N_c) to take into account when computing the numerical periodic Green function. Indeed as in this case we are using the Green functions of a stratified half-space we were not able to use the convergence results given in Sect. 4.1. On Fig. 8 we have plotted the moduli of c_I for $N_c = 8$ and $N_c = 13$ at low and high frequencies. The value $N_c = 8$ was adopted despite the difference on the fifth mode at high frequency and the following results are then provided when 17 panels ($2N_c + 1$) were taken into account. Results in the frequency domain show that the most active participation factors are those corresponding to a flexural mode of the plate in the e_1 direction which is the loading polarisation. Moreover the moduli of these participation factors decrease when the mode number increases. We have chosen here some interesting participation factors. For example, the effect of water on the seismic behaviour of the quay wall can be seen on Fig. 9 where we plot the moduli of two participation factors (c_4 and c_5) versus the frequency in the two cases AW (black lines) and AN (grey ones). The responses are quite similar except for some resonance frequencies where the AW responses are higher. In fact near resonance frequencies one can easily show that the modulus of a frequency response function is proportional to the mass. The presence of water bringing additional mass to the system, case AW responses are higher than case AN ones. The effect of anchors can be seen on Fig. 10 where we compare cases AW and FW responses. These have quite similar shapes, the free panel response (dark curves)

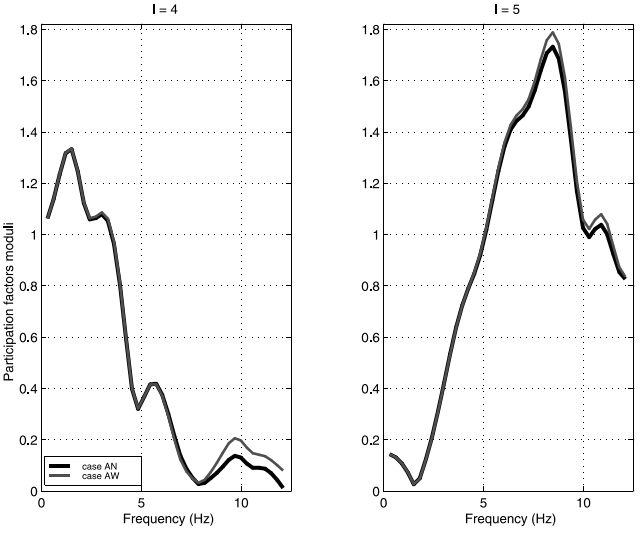

Fig. 9. The effect of water on some participation factors

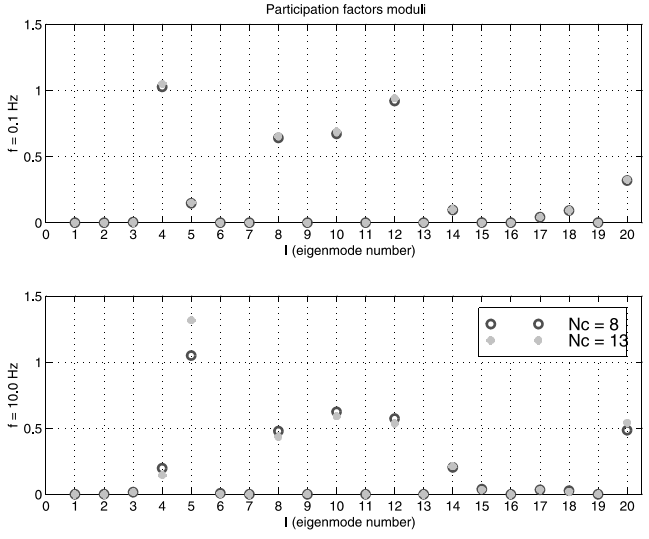

Fig. 8. Participation factors ($\{c_I\}_{I=1,20}$) convergence

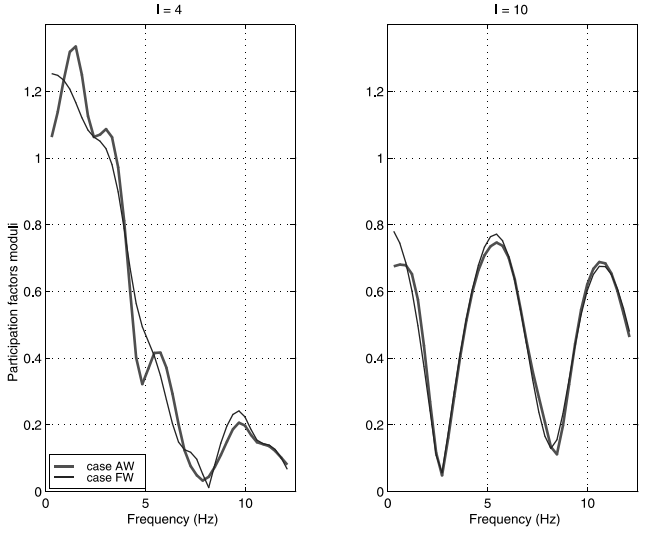

Fig. 10. The effect of anchors on some participation factors

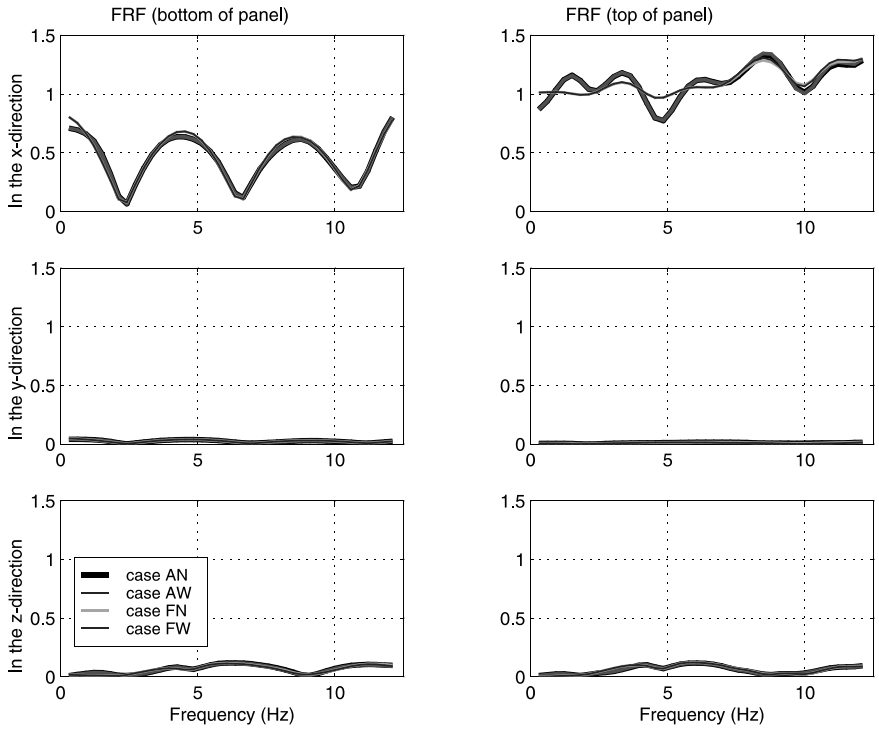

Fig. 11. Displacement FRF on top and bottom of the panel in the e_1 (x) e_2 (y) and e_3 (z) directions

being smoother than the anchored panel one where the perturbations are due to the presence of the 8 anchors in the soil. Concerning the displacement, we show the Frequency Response Functions at the top and at the bottom of the panels in the four studied cases (Fig. 11). These FRF are normalized using the displacement at the top of the layer which explains the disamplifications of the bottom displacement curves. We notice that the e_1 direction is the most active one because it is the loading excitation direction.

6 Conclusion

We have presented in this paper a periodical approach coupling finite elements and boundary elements even for non periodic loadings. The case of stochastic loading has been presented in another paper [15]. Moreover, the efficiency of this approach has been proven and several validation tests shown. We have applied this new methodology to model a dynamic soil-quay wall intercation and we compared several configurations of the quay-wall under a vertically propagating plane wave. Convincing results have been obtained.

References

1. **Abboud T, Mathis V, Nedelec J-C** (1995) Diffraction of an electromagnetic travelling wave by a periodic structure. In: Cohen G et al., (ed.) Third international conference on Mathematical and Numerical Aspects of Wave Propagation. SIAM, 1995
2. **Aubry D** (1986) Sur une approche intégrée de l'interaction sismique sol-structure. Revue Française de Géotechnique 38: 5–24
3. **Aubry D, Clouteau D** (1991) A regularized boundary element method for stratified media. In: Cohen G, Halpern L, Joly P (eds.) Mathematical and numerical aspects of wave propagation phenomena, Proc. 1st Int. Conf., Strasbourg, France, 23–26 April 1991, pages 660–668, SIAM, Philadelphia, INRIA, SIAM
4. **Aubry D, Clouteau D** (1992) A subdomain approach to dynamic soil-structure interaction. In: Davidovici V, Clough R (eds.) Recent advances in earthquake engineering and structural dynamics, pages 251–272. Ouest Editions/AFPS, Nantes
5. **Bensoussan A, Lions JL, Papanicolaou G** (1978) Asymptotic analysis for periodic structures. North–Holland, Amsterdam
6. **Bonnet M** (1999) Boundary integral equations methods for Solids and Fluids. John Wiley and Sons
7. **Bossavit A** (1986) Symmetry, groups and boundary value problems: a progressive introduction to non commutative harmonic analysis of partial differential equations in domains with geometrical symetry. Comp. Meth. in Appl. Mech. Eng. 56: 167–215
8. **Brebbia CA**, editor (1996) The Kobe earthquake geodynamical aspects. Computational Mechanics Publications
9. **Brillouin L** (1953) Wave propagation in periodic structures. Dover
10. **Cascone E, Maugri M** (1995) On the seismic behavior of cantilever retaining walls. In Proc. of the tenth ECEE conf. Balkema
11. **Chang O, Liao J, Lin H** (1998) Performance of diaphragm wall using top-doen method. J. Geothenical Geoenvironmental Eng.
12. **Chen X, Fiedman A** (1991) Maxwell's equations in a periodic structure. Trans. Amer. Math. Soc. 323: 465–507
13. **Clouteau D** (1990) Propagation d'ondes dans des milieux hétérogènes, Application à la tenue d'ouvrages sous séismes. PhD thesis, Ecole Centrale de Paris
14. **Clouteau D, Aubry D** (1993) 3d seismic soil-fluid-structure interaction for arch dams including source and site effects. In Proc. of Eurodyn93 Int. Conf., pages 1217–1224, Rotterdam, Balkema
15. **Clouteau D, Aubry D, Elhabre M, Savin E** (1999) Periodic and stochastic bem for large structures embedded in an elastic half-space. Mathematical aspects of boundary element methods, pp 91–102

16. **Clouteau D, Devesa G, Jacquart G** (1999) Couplage FEM-BEM: applications pratiques en génie parasismique. In: Ladevèze P, Guedra Degeorges D, Raous M (ed.) Actes 4ème Colloque National en Calcul des Structures, Giens, France, 18–21 Mai 1999, vol. 1, pp. 215–220, Teknea, Toulouse
17. **Colton D, Kress R** (1983) Integral equation methods in scattering theory. Pure and applied Mathematics. Wiley and Sons
18. **Craig R, Bampton M** (1968) Coupling of substructures for dynamic analysis. AIAA J. Aircraft 6(7): 1313–1319
19. **Elhabre M** (1999) Interaction sismique Sol-Fluide-Structure. PhD thesis, Ecole Centrale de Paris
20. **Elhabre M-L, Clouteau D, Aubry D** (1998) Sesmic behavior of diaphragm walls. In: Bisch P (ed.) 11th European conference on earthquake engineering, Rotterdam, September, Balkema
21. **Floquet MG** (1883) Sur les équations différentielles linéaires à coefficients périodiques. Annales de l'Ecole Normale, 12
22. **Mahadevan K** (1996) Edge-based finite element analysis of singly- and doubly-periodic scatterers using absorbing and periodic boundary conditions. Electromagnetics 16: 1–16
23. **Pozrikidis C** (1996) Computation of periodic Green's functions of stokes flow. J. Eng. Mathematics 30: 79–96
24. **Sanchez-Hubert J, Turbe N** (1986) Ondes élastiques dans une bande périodique. Mathematical Modelling and Numerical Analysis 30(3): 539–561
25. **Savin E** (1999) Effet de la variabilité du sol et du champ incident en interaction sismique sol-structure. PhD thesis, Ecole Centrale de Paris